Experimental Comparison of Acoustic Characteristics for a High-Efficiency Magnetic Gearbox and a Mechanical Planetary Gearbox for Industrial HVAC Applications

Guanhua Tao, Bryton Praslicka, *Graduate Student Member, IEEE,* Shima Hasanpour, *Graduate Student Member, IEEE*, Thomas Simms*, Student Member, IEEE,* Zakki Wibisono, Matthew C. Gardner, *Member*, Matthew Johnson, *Member*, Emily Hankins, Maggie McCall, Alinoe Roussie, Samuel Ortiz, William Thiele, Hamid A. Toliyat, *Fellow, IEEE.*

***Abstract*—In industrial fan applications, gearboxes or belt drives are often utilized to reduce the motor footprint to an acceptable level to maximize airflow. Customers demand fans with minimal noise and maintenance requirements, as well as a large mean time to failure (MTTF); however, mechanical gearboxes and belt drives are associated with high noise levels, significant maintenance requirements, and low MTTF rates, especially in harsh environments. This paper presents the development of a radial flux coaxial magnetic gear optimized for cost and modulator retention. The results reveal that sizable retaining features on the modulators' tangential sides may be employed while still maintaining high electromagnetic performance. A magnetic gear prototype was constructed and evaluated to determine its A-weighted acoustic noise characteristics. A similar commercial-off-the-shelf mechanical planetary gearbox was also evaluated to provide a benchmark for comparison with the magnetic gearbox. The results reveal the novel finding that the magnetic gearbox became quieter as the load increased, and the mechanical gearbox was louder than the magnetic gearbox at rated speed, except at very light loads. A second magnetic gearbox was also tested and proved to be louder than the mechanical gearbox; however, this second magnetic gearbox also became quieter as its load increased.**

***Index Terms*—Unbalanced forces, magnetic forces, vibration, acoustic noise, magnetic gear**

I. Introduction

INDUSTRIAL fans used in heating, ventilation, and air conditioning (HVAC) applications typically employ 2 or 4 pole motors with belt drives to achieve the desired fan speeds of 300-600 rpm, as direct drive solutions often possess a larger footprint [1], [2]. However, belt drive solutions are also associated with high maintenance costs, low reliability, and low transmission efficiency [1], [2]. Mechanical gears in air-cooled condenser fans also generally exhibit a low mean time to failure (MTTF) [3]. Moreover, teeth meshing in mechanical gears can emit high volume noise. For example, rotorcraft commercial adoption is hindered by excessive cabin noise (often exceeding 100 dB), caused primarily by structural vibrations originating from the main rotor gearbox meshing [4].

Magnetic gears convert energy between low-speed, high-torque rotation and high-speed, low-torque rotation. Like mechanical gears, magnetic gears allow a relatively small, high-speed electric machine to connect to a low-speed, high-torque system. Magnetic gears transfer power through modulated magnetic fields instead of the meshing teeth used in mechanical gears. Magnetic gears' contactless operation provides a plethora of potential benefits, such as improved reliability, reduced maintenance, reduced acoustic noise, and physical isolation between shafts. Thus, magnetic gears have generated significant interest, leading to the development of some magnetic gear prototypes for HVAC applications [2], [3].

Radial flux coaxial magnetic gears, such as the one shown in Fig. 1, have demonstrated the highest experimental magnetic gear torque densities reported to date [5]-[7]. In a coaxial magnetic gear, the number of modulators on Rotor 2 (Q_2) should be the sum of the pole pairs on Rotor 1 (P_1) and Rotor 3 (P_3), as in

$$Q_2 = P_1 + P_3. \tag{1}$$

Magnetic gears have different operating modes, which yield different gear ratios. However, the highest fixed gear ratio is achieved when the high pole count PM rotor (Rotor 3) is held

Funding provided in part by the National Security Innovation (NSIN) Capstone Project Program.

B. Praslicka, S. Hasanpour, T. Simms, Z. Wibisono, and H. A. Toliyat are with the Advanced Electric Machines and Power Electronics Lab at Texas A&M University, College Station, TX 77843 USA (e-mail: bryton.praslicka@tamu.edu, shimahasanpour@tamu.edu, tasimms33@tamu.edu, zakkiboi@tamu.edu, toliyat@tamu.edu).

G. Tao, E. Hankins, M. McCall, A. Roussie, S. Ortiz, W. Thiele are with the J. Mike Walker '66 Department of Mechanical Engineering at Texas A&M University, College Station, TX 77843 USA (e-mail: guanhua_tao@tamu.edu, emilyhankins5@tamu.edu, maggiemccall14@tamu.edu, alinoe.r1@tamu.edu, samortiz12@tamu.edu, wthiele99@tamu.edu)

M. Johnson was with the DEVCOM Army Research Laboratory, College Station, TX 77843 USA (e-mail: matthew.c.johnson186.civ@army.mil).

M. C. Gardner is with the Electric Powertrains Lab at the University of Texas at Dallas, Richardson, TX 75080 USA (e-mail: Matthew.Gardner@utdallas.edu).

stationary, yielding the gear ratio given by

$$\text{Gear Ratio} = \frac{\omega_1}{\omega_2} = \frac{Q_2}{P_1}, \quad (2)$$

which relates the steady-state speeds of Rotor 1 (ω_1) and Rotor 2 (ω_2).

Due to the technology's relative immaturity, some previous magnetic gear prototypes exhibited undesirable characteristics, such as vibrations due to unbalanced magnetic forces [3], [5], [8]-[10], significant deflection of the modulators, modulator housing [11], [12], or inner rotor/stator [13], or other structural deficiencies that result in high noise levels [14], [15]. Additionally, relatively few magnetic gear experimental vibration analysis studies have been conducted [9], [10], [15]. Some theoretical studies on deflection [12], [16] and vibration [15], [17]-[19] exist but make significant limiting assumptions, such as lumping rotors into one rigid body [17].

This paper presents the design, construction, and experimental analysis of a magnetic gear prototype optimized for cost for an HVAC application. The authors' experience informed the modulator cage assembly design, which is made of a specially formulated plastic with a high elastic modulus to avoid modulator rotor deformation. For commercial prototype samples, the gear was designed to be integrated into the National Electrical Manufacturer Association (NEMA) 182-frame housing with a 4-pole, 6 HP motor. However, for experimentation, a standalone magnetic gear with identical magnetically active parameters was also fabricated. This paper describes a carefully designed experiment intended to capture the effects of loading on the vibrational responses of mechanical and magnetic gears. This paper also presents static and dynamic experimental results for the magnetic gear prototype. The A-weighted and unweighted sound pressure of the mechanical and magnetic gear are compared. The results reveal that even a magnetic gear with static rotor eccentricity, which causes significant low frequency vibrations, produces lower acoustic noise than a comparable commercial-off-the-shelf mechanical planetary gearbox at many loads and speeds.

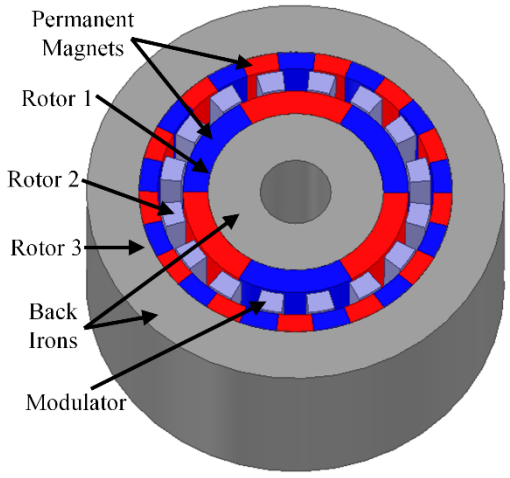

Fig. 1. Example radial flux coaxial magnetic gear.

II. Design Study Methodology

The coaxial magnetic gear was designed to replace a planetary gearbox used in an existing commercial HVAC application, which employs a 4-pole motor. Table I summarizes the gear's dimensional constraints and performance specifications. An extensive parametric 2D finite element analysis (FEA) study was performed to evaluate various design combinations. Table II shows the design parameters and values considered in this study, including some derived parameters. The first derived parameter is the PM thickness ratio (k_{PM}), which relates the thickness of the magnets on Rotor 3 (T_{PM3}) to the thickness of the magnets on Rotor 1 (T_{PM1}) according to

$$T_{PM3} = k_{PM} T_{PM1}. \quad (3)$$

Based on the operating temperature, supplier availability for manufacturing at scale, and the competitive price of $0.10 per gram, N45UH was chosen for all PMs. This selection was made by using the lookup table presented in [20] and then validated via FEA simulation. 29-gauge M15 electrical steel with C5 coating was used for the back irons and the modulators.

To avoid unbalanced magnetic forces and excessive torque ripple, proper pole pair selection is critical, as explained in [5]. Based on [5], G_{Int} is used to represent the integer part of the gear ratio defined in (2) and the Rotor 3 pole pair count is given by

$$P_3 = \begin{cases} (G_{Int} - 1)P_1 + 1 & \text{for } G_{Int}P_1 \text{ odd} \\ (G_{Int} - 1)P_1 + 2 & \text{for } G_{Int}P_1 \text{ even} \end{cases} \quad (4)$$

TABLE I
Magnetic Gearbox Target Specifications

Constraint/Specification	Value	Units
Active material outer diameter	146.05	mm
Output speed	540-600[a]	rpm
Continuous torque rating	60	N·m
Ambient operating temperature	60	°C
Total[b] axial length	50.8	mm

[a]The upper output speed range was most preferable for the end application.
[b]Including structural components and nonconductive nonmagnetic buffer.

TABLE II
Design Parameter Sweep Ranges

Description	Value	Units
Integer part of the gear ratio (G_{Int})	2, 3	
Rotor 1 pole pair count (P_1)	3, 4, 5, 6, 7	
Active outer radius (R_{Out})	73.025	mm
Air gap thickness (T_{AG})	0.5, 0.75, 1	mm
Rotor 1 back iron thickness (T_{BI1})	5, 10, 15	mm
Rotor 3 back iron thickness (T_{BI3})	5, 10	mm
Modulators thickness (T_{Mods})	6, 8, 10, 12	mm
Modulators bridge thickness (T_B)	0, 0.5, 1.0	mm
Rotor 1 PM thickness (T_{PM1})	6, 8, 10, 12	mm
PM thickness ratio (k_{PM})	0.5, 0.75, 1	
Rotor 1 PM tangential fill factor (α_{PM1})	0.91, 1	
Rotor 3 PM tangential fill factor (α_{PM3})	0.95, 1	

As explained in [5], proper pole pair count selection is the most important design consideration to reduce a magnetic gear's torque ripple. The final magnetic gear design's slip torque was selected to ensure that the gear would not slip during start-up with a large inertial load [2], [21], [22].

III. Design Study Simulation Results

Permanent magnet material is the primary driver of material costs in most magnetic gears [23]. Thus, PM torque density can be used as a metric for optimization. PM torque density is defined as the low-speed rotor's slip torque divided by the design's total PM mass. The highest PM torque density designs generally favor the largest possible outer radius. Consequently, only designs with the maximum allowable outer radius of 73.025 mm (corresponding to a 5.75 in diameter) were considered. Rotor 2 was used as the low-speed output rotor, allowing a lower Q_2 than if the same gear ratio was achieved with Rotor 3 as the low-speed rotor. This reduced Q_2 yields more manufacturable and structurally robust modulator pieces with longer arc lengths.

A. Broad Parametric Analysis

Fig. 2 presents some design trends ascertained from the parametric design study described by Table II. Fig. 2(a) reveals that it is generally optimal for the Rotor 1 magnets to be thicker than the Rotor 3 magnets. This is because Rotor 3 has more poles than Rotor 1; hence, Rotor 3 experiences more flux leakage between adjacent poles. Fig 2(a) also reveals that designs optimized for PM torque density possess thinner magnets. Both of these observations agree with [24]. While radially thicker modulators or a modulator bridge can structurally strengthen the modulator assembly, Fig. 2(b) shows that thinner modulators generally yield higher PM torque densities, which also agrees with [24]. Fig. 2(b) also shows that a modulator bridge reduces the torque capacity of a magnetic gear design, which is in concordance with [25], [26].

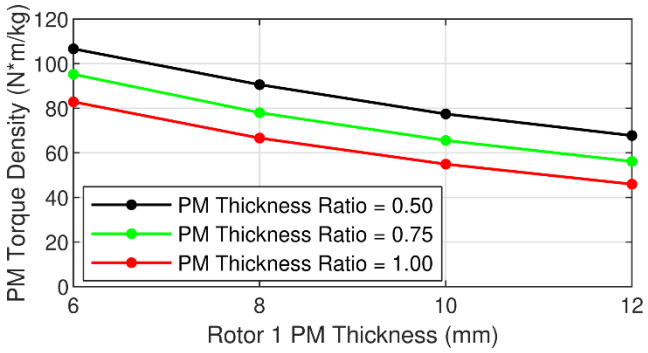

(a)

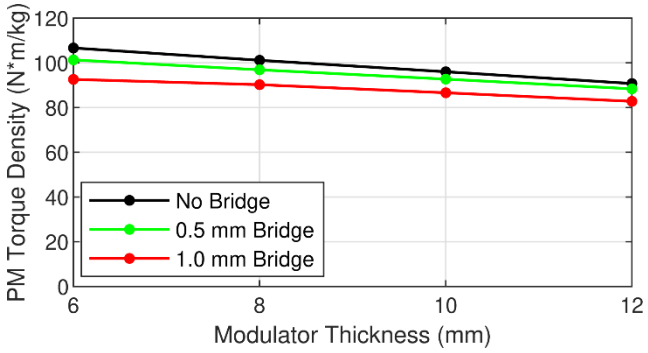

(b)

Fig. 2. PM torque density variation with (a) Rotor 1 PM thickness and the PM thickness ratio and with (b) modulator thickness and modulator bridge thickness.

Ultimately, parameters such as magnet and modulator thicknesses were selected based on the trade-off between magnetic performance, structural integrity, manufacturing costs, and raw material costs. 3D transient FEA simulations revealed that ~16 mm (5/8 in) of axial buffer space is required on each end of the gear to ensure that the eddy currents induced in the structural materials would be negligible [27].

B. Parametric Optimization of Modulator Shape

The magnetic gear uses modulator grooves for structural support, as shown in Fig. 3. Once most of the final parameter values were selected, a thorough parametric optimization of the modulator shape was performed. Consider a modulator with average arc length, S, tangential groove depth, δ, and groove radial thickness, r, as shown in Fig. 3. The groove tangential fraction, k_{tan}, is the groove tangential depth normalized by half of the modulator arc length, as given by

$$k_{tan} = \frac{2\delta}{S}. \tag{5}$$

The groove radial fraction, k_{rad}, represents the fraction of the modulator radial thickness eliminated by the groove at the modulator's tangential edge and it is given by

$$k_{rad} = \frac{r}{T_{Mods}}. \tag{6}$$

The parametric modulator designs study evaluated different modulator radial thicknesses and groove dimensions, as well as different modulator inner and outer tangential fill factors between 0.50-0.65 and 0.50-0.775, respectively. This resulted in 14,790 different modulator geometries that were evaluated in the modulator design study. Fig. 4 presents some of this study's results and shows that a high PM torque density is achievable even with sizable grooves cut into the modulators. However, at high k_{rad} and k_{tan} values, saturation begins to occur in the thin corners of the modulator pieces. Additionally, at higher k_{tan} values, the tangentially thin center of the modulator pieces saturates, which lowers the PM torque density. Some optimal

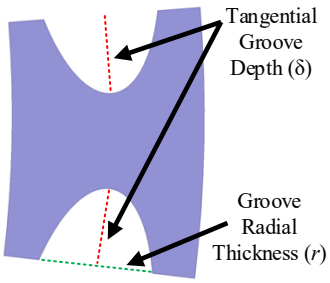

Fig. 3. Annotated grooved modulator pole piece.

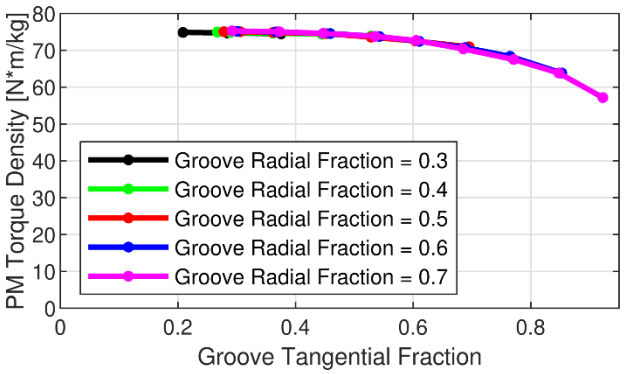

Fig. 4. Variation of maximum achievable PM torque density with modulator groove design parameters.

modulator designs were also structurally analyzed. Based on this study and practical considerations, a modulator design characterized by k_{rad} = 0.7, k_{tan} = 0.2, and 50% inner and outer tangential fill factors was chosen for the final prototype, because these parameters yielded acceptably high PM torque density and structural integrity. Notably, using these grooved modulators reduced the peak-to-peak torque ripple on the modulators from 1.2% to 1.0% of the average modulator torque (as compared to the corresponding design using ideal annular segment modulators). Similarly, using these grooved modulators reduced the peak-to-peak torque ripple on the high-speed rotor from 3.4% to 2.0% of the average high-speed rotor torque (as compared to the corresponding design using ideal annular segment modulators).

IV. Experimental Testbed Development

This section describes the design of the experimental testbed used to evaluate the magnetic and mechanical gearboxes. Fig. 5(a) contains a SolidWorks rendering of the testbed. Fig. 5(b) shows a picture of the experimental testbed, including the dynamometer and anechoic chamber. Fig. 5(c) shows a rendering of the anechoic chamber with annotations indicating the relative positions of the microphones and the magnetic gear prototype, which is the device under test (DUT). This indicates the distances between the sound radiating body and the sound measurement devices.

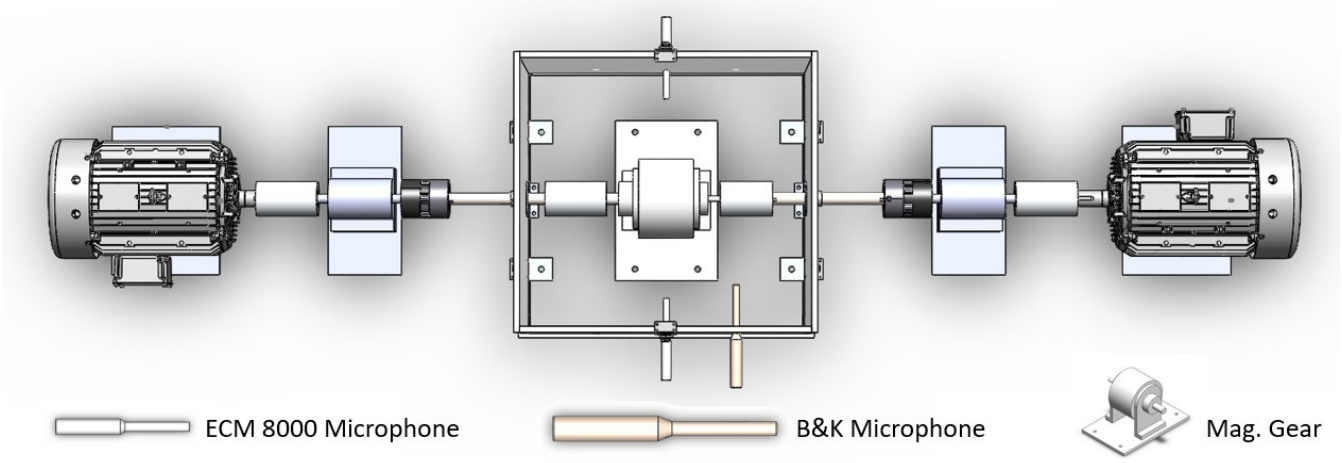

(a)

(b)

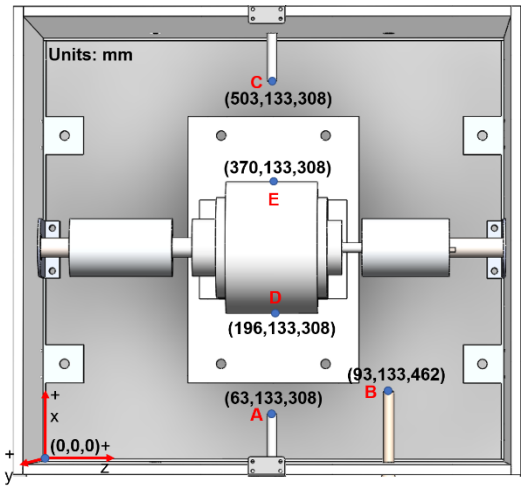

(c)

Fig. 5. (a) A computer aided design (CAD) conceptual rendering of the experimental dynamometer with gearbox anechoic chamber and the microphones used for acoustic measurements. (b) The actual physical testbed. (c) A rendering of the anechoic chamber with annotations indicating the relative positions of the microphones and the magnetic gear, which is the device under test (DUT).

The prototype 1800 rpm NovaMAX® 215 frame size motor described in [28] served as the prime mover. A Yaskawa A1000 variable frequency drive (VFD) operating at a switching frequency of 4 kHz was used to the drive motor. During initial testing, the switching frequency of the drive was varied between 4 kHz and 10 kHz to determine if switching frequency appeared in the acoustic signature of the magnetic gear, but as expected, it did not. A Marathon Black Max induction generator served as the mechanical load. The generator was controlled by a Yaskawa U1000 VFD. The torque and speed on the gearbox's input and output shafts were measured by two Himmelstein MCRT 49802V torque meters. These measurements were used to calculate the mechanical power entering and exiting the gearbox. Steel helical couplings were used instead of jaw couplings to connect the shafts inside of the anechoic chamber. This decision minimized the noise radiating from the couplings; however, it also only allowed experimental data to be collected for torques of up to ~15 N·m on the low-speed rotor due to the helical coupling's dynamic rating.

The sound pressure data was collected through two ECM8000 Ultra-Linear Condenser Studio Microphones with relatively flat frequency responses via XLR cables connected through a Behringer UMC202HD interface. The sound pressure data was recorded in the free Audacity digital audio workstation software using 24-bit depth and a 44,100 Hz sampling rate. These two microphones were employed to measure unweighted sound intensity on a normalized scale, with 1 per unit (p.u.) corresponding to 0 Decibels relative to full-scale (dBFS), in order to generate clean, relatively noise-free waterfall plots. The acoustic data captured using the linear frequency response microphones are critical for validating noise, vibration, and harshness (NVH) simulation models and for determining the coaxial magnetic gear's equivalent radiated power. The A-weighted sound pressure level (SPL) was also logged with a Brüel & Kjær (B&K) 2230 sound level meter to provide insight into how the human ear might experience the radiated acoustic power. Fig. 5(c) shows the 3D coordinates of the three microphones and the coaxial magnetic gear DUT to indicate the distances between the sound radiating body and the sound measurement devices.

The acoustic noise radiated by mechanical gears typically increases as their load increases, as a result of gear whine, which may increase with load [29], [30]. Gear whine refers to noise produced by vibrations resulting from meshing stiffness variation, manufacturing error, and tolerance error [29], [30]. Experimental data was collected to capture the effect of load on a magnetic gear's vibrationally radiated power, which generates acoustic noise. The experimental data was obtained using the following process:

1. Start with the minimum speed and then increase the high-speed rotor input speed in 30 rpm steps.
2. At each new speed, wait for the torque measurement to reach steady-state before collecting a data sample and changing the speed again.
3. When post-processing the data, determine the start of each acceleration/deceleration event and use a 3 s sample of data corresponding to the interval starting 4.5 s before the event and ending 1.5 s prior to it.

The 3 s sample of acoustic data prior to each acceleration event, which isolates each steady-state speed and load torque, is the data used for analysis. Fig. 6 illustrates the selection of these data subsets that were used for analysis.

V. Experimental Results

A. Coaxial Magnetic Gearbox Torque and Efficiency

Table III lists the dimensions of the coaxial magnetic gear prototype, and Fig. 7 shows the magnetic gear prototype inside of its aluminum housing. The magnetic gear prototype's experimentally measured slip torque was 65 N·m at room temperature, about 3% lower than the slip torque predicted by an FEA simulation. Figs. 8(a) and 8(b) show the loss data and corresponding efficiency values for the magnetic gear prototype as a function of input speed and load torque. Due to coupling ratings, only output torques of 15 N·m or less were measured dynamically, so only the portions of the contour plots below the red curves in Figs. 8(a) and 8(b) correspond to experimentally

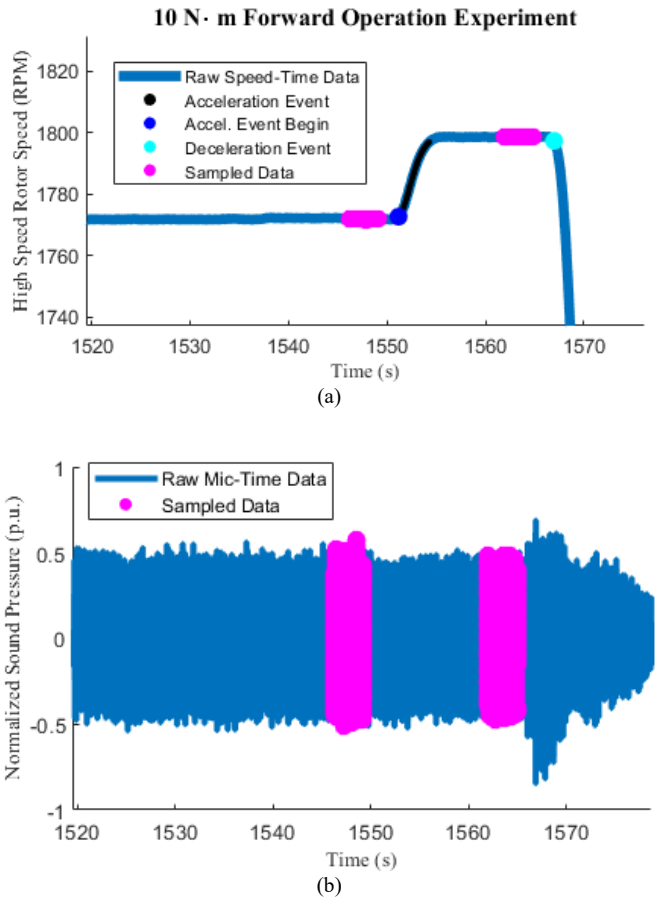

Fig. 6. Experimentally measured (a) input speed data and (b) the corresponding microphone data collected during an acceleration event and a deceleration event with a constant 10 N·m load on the output rotor. The sampled microphone data used to characterize a steady-state operating point's acoustic noise is indicated by the magenta markers and corresponds to the 3 s interval that starts 4.5 s before an acceleration or deceleration event and ends 1.5 s before the event.

TABLE III
PROTOTYPE COAXIAL MAGNETIC GEARBOX
MAGNETICALLY ACTIVE DESIGN PARAMETERS

Parameter	Value	Units
Active material outer radius	73	mm
Gear ratio	3.2	
Inner rotor magnet thickness	10	mm
Inner and outer air gap effective thicknesses[a]	0.75	mm
Modulator radial thickness	8	mm
Outer rotor magnet thickness	5	mm
Outer back iron yoke thickness	10	mm
Magnetically active stack length	34.9	mm
Total[b] axial length	66.7	mm

[a]Including carbon fiber retaining sleeve used in production.
[b]Including nonconductive nonmagnetic buffer space.

Fig. 7. Coaxial magnetic gear prototype.

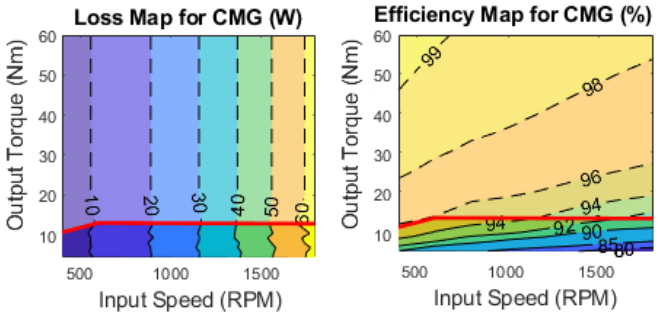

(a) (b)

Fig. 8. Coaxial magnetic gear (CMG) (a) losses and (b) efficiency variation with input speed and output torque load., from directly measured. Efficiency and losses were experimentally measured for loads ranging from 5 N·m to 13.01 N·m. Efficiency and loss characteristics above the red curves were extrapolated from the experimental data based on the assumption that losses are invariant with torque load.

measured data. However, the experimental data indicate that the magnetic gear losses primarily depend on operating speed and not on load torque, which agrees with the behavior observed in [26], [31]-[33]. This is because the permanent magnets are always on, regardless of the torque load, and the dominant loss sources are windage, hysteresis, and eddy currents, all of which are speed dependent. The portions of the contour plots above the red curves in Figs. 8(a) and 8(b) are based on extrapolation of the experimental data up to rated torque, using the assumption that the losses are invariant with respect to load torque and thus remain constant at a given speed. At a 400 rpm input speed and a 60 N·m output torque, FEA simulation results predicted a peak electromagnetic efficiency of 99.24%. Extrapolation of the experimental results to the same operating point predicts an efficiency of 98.21%. These high efficiency values are generally consistent with the high experimental efficiency values recorded in [32], which provides more detail on the losses breakdown for the magnetic gear prototype used in that study. Losses in the modulators are reduced in both magnetic gear prototypes in part by laminating the modulators.

B. Acoustic Benchmarking Against Mechanical Gearbox

A Neugart PLE080-003-SFSA3AE-R19 mechanical gear with a carrier output [34] was selected to provide a benchmark comparison with the magnetic gear protype. Table IV lists the mechanical planetary gearbox's relevant design and performance parameters. Fig. 9 shows a plot of the RMS A-measured weighted decibel sound pressure data for both the coaxial magnetic gear and the mechanical planetary gear. These measurements reveal that the mechanical gearbox's acoustic noise increases slightly with load. This is likely a result of gear whine. At no load and high speeds, the slight increase in the mechanical planetary gear's acoustic noise is a result of gear rattling. Gear rattling is a problem with many automotive transmissions [35], which endure repetitive impact between gears due to vibrations made possible by the gearbox's backlash. The results shown in Fig. 9 also reveal that the magnetic gear becomes acoustically quieter as the load increases, while operating at a constant rated speed of 1800 rpm on the high-speed rotor. Of note, at almost all speeds, when under a 15 N·m load, which is less than 25% of the magnetic gear's slip torque, the magnetic gearbox is quieter than the mechanical gearbox.

C. Acoustic Testing of a Second Coaxial Magnetic Gear Prototype

To further substantiate the magnetic gear acoustic characteristic trends, a second coaxial magnetic gear prototype was tested using the same experimental setup as the first magnetic gear prototype. This second magnetic gear prototype is a retrofitted and reconstructed version of the magnetic gear described in [32], which uses Halbach arrays and air cores. Fig. 10 shows the second prototype in its 3D printed housing, while Table V lists some of its key geometric design parameters.

Fig. 12 presents the RMS A-weighted decibel sound pressure data recorded at different operating speeds under three distinct loading conditions: 0 N·m, 5 N·m, and 10 N·m. The experimental results for this second magnetic gear prototype

TABLE IV
MECHANICAL GEARBOX[a] PARAMETERS AND RATINGS [34]

Parameter	Value	Units
Nominal Output Torque Rating	85	N·m
Nominal Input Speed Rating	4000	rpm
Housing Diameter	80	mm
Housing Axial Length (excluding shaft)	60	mm
Gear Ratio	3:1	–
Number of Gearbox Stages	1	–
Coordinates of Radial Surface Point Analogous to Point D in Fig. 5(c)	(243, 133, 308)	mm
Coordinates of Radial Surface Point Analogous to Point E in Fig. 5(c)	(323, 133, 308)	mm

[a]The mechanical gearbox is a NEUGART PLE080-003-SFSA3AE-R19 [34].

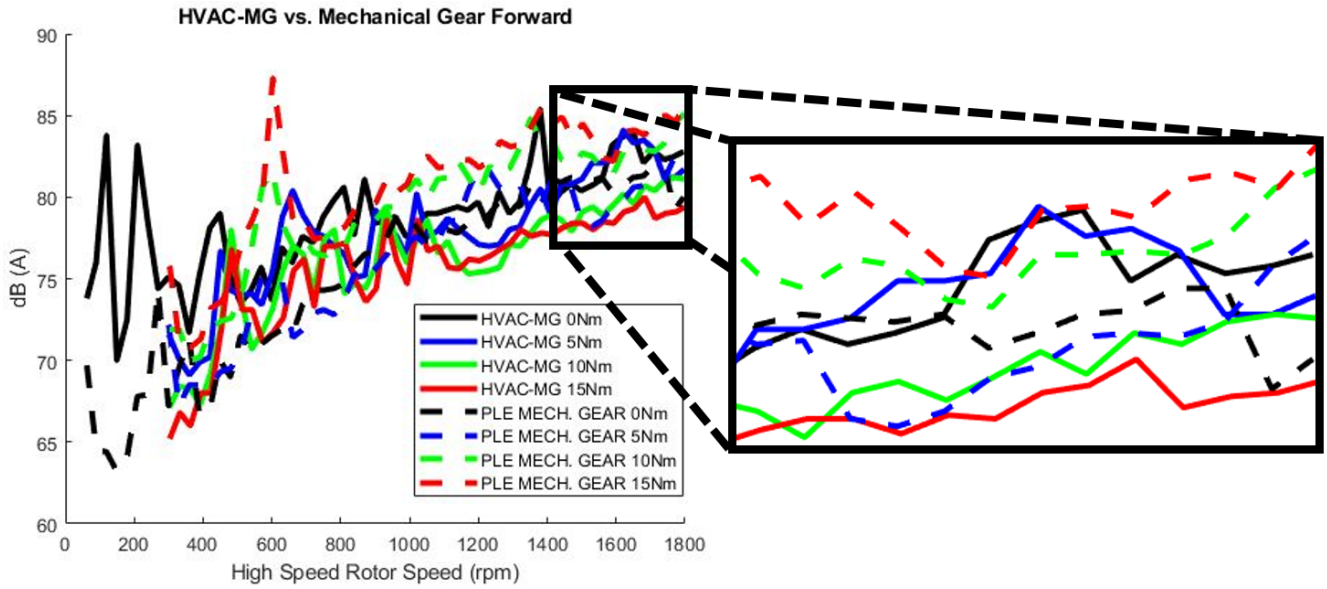

Fig. 9. A-weighted rms sound pressure from the prototype magnetic gear (HVAC-MG) and the benchmarking mechanical gear (PLE MECH. GEAR) under steady-state operating conditions over a range of input speeds and load torques.

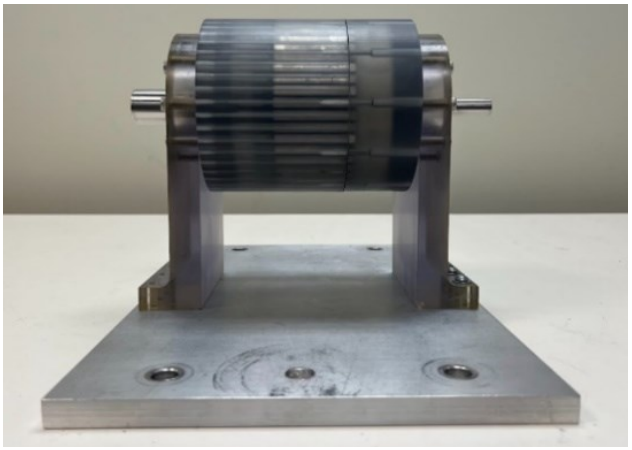

Fig. 10. Second coaxial magnetic gear prototype.

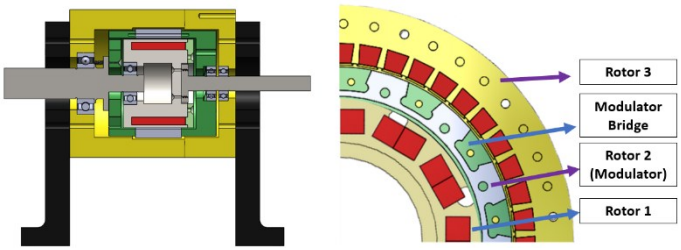

Fig. 11. Mechanical and electromagnetic design cross-sections of the second coaxial magnetic gear prototype.

agree with the trend demonstrated by the results for the first magnetic gear prototype: the magnetic gear's acoustic noise decreases as its load torque increases. This is the opposite of the trend seen in the mechanical gear's experimental results, which exhibit an increase in acoustic noise as the load torque increases.

TABLE V
PARAMETERS AND RATINGS FOR THE SECOND COAXIAL MAGNETIC GEAR PROTOTYPE [32]

Parameter	Value	Units
Number of Rotor 1 pole pairs	3	--
Number of modulators	14	--
Number of Rotor 3 pole pairs	11	--
Number of PM pieces per Rotor 1 pole	2	--
Number of PM pieces per Rotor 3 pole	2	--
Number of parts per pole of Rotor 1 magnet poles	2	--
Number of parts per pole of Rotor 3 magnet poles	1	--
Outer radius of Rotor 3 PMs	50.8	mm
Outer air gap physical air gap thickness	1/8	in
Radial thickness of Rotor 3 PMs	1	mm
Radial thickness of Rotor 2	7.5	mm
Radial thickness of bridge	1.5	mm
Inner physical air gap thickness	0.96	mm
Radial thickness of Rotor 1 PMs	0.25	in
Tangential width of Rotor 1 PMs	0.25	in
Tangential width of Rotor 3 PMs	0.125	in
Maximum sleeve radial thickness between air gap and rotor 3 PMs	2.36	mm
Maximum sleeve radial thickness between air gap and rotor 3 PMs	1.77	mm
Modulators fill factor at the Rotor 2 outer radius	0.5	--
Modulators fill factor at the Rotor 2 inner radius	0.7	--
Radius of modulator holes	1.2	mm
Axial length of Rotor 3 PMs	2	in
Axial length of modulators	37.8	mm
Axial length of Rotor 1 PMs	1.750	in
Material for rotor housing	Accura 60	--

VI. Conclusion

Cost, reliability, efficiency, and acoustic noise are all critical aspects to consider when designing magnetic gears. Magnetic gears have been proposed as an alternative to belt drives or

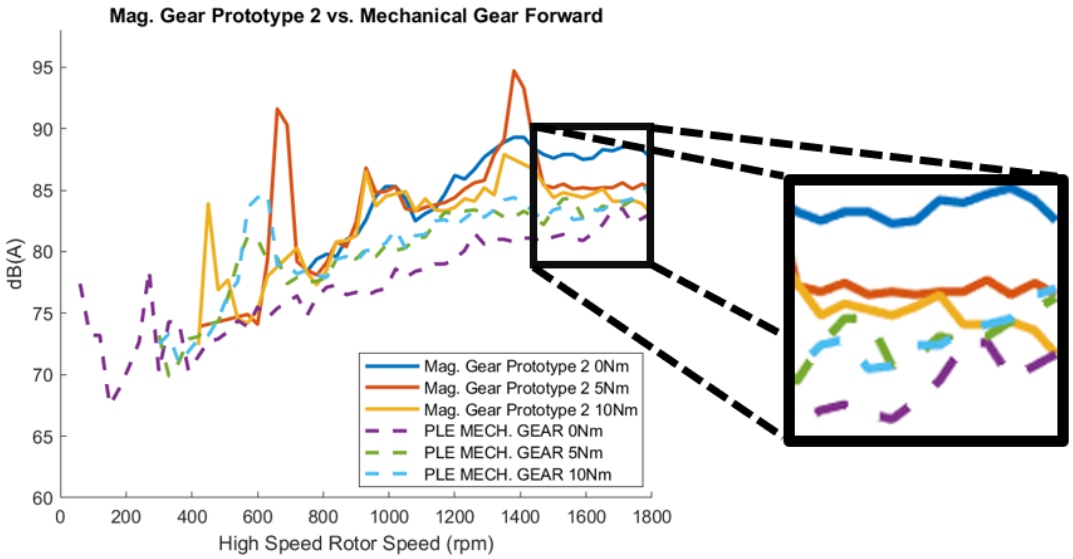

Fig. 12. A-weighted rms sound pressure from the second magnetic gear prototype under steady-state operating conditions over a range of input speeds and load torques.

mechanical gearboxes for HVAC applications because of their potential for an increased mean time to failure (MTTF) and reduced acoustic noise. To minimize cost, a thorough parametric analysis was conducted using 2D FEA simulations. Special attention was given to the modulators to select a shape that provides both good mechanical interlocking features and good electromagnetic torque transmission capabilities.

Grooved modulator designs allow good mechanical interlocking (Fig. 3) with negligible negative impact, or even a slight positive impact on the design's electromagnetic torque transmission capability (Fig. 4). Additionally, while previous authors conducted some preliminary noise and vibration analyses, to date, no study has discussed the effects of loading or designed a proper NVH test apparatus with vibro-acoustic isolation. An acoustic chamber was created (Fig. 5) and used to capture experimental acoustic data measurements. A second coaxial magnetic gear prototype, which is a retrofitted and reconstructed version of the magnetic gear described in [32] was also tested. The resulting experimental acoustic data for this second magnetic gear prototype was compared to measurements obtained from the HVAC magnetic gear. This comparison is visualized in Figs. 10 and 12, which contrast the acoustic noise characteristics of these two magnetic gears against those of a mechanical gear. Based on these results, this paper makes the following novel contributions to the existing literature:

- These are the first known comparisons of the noise characteristics for a magnetic gear and a mechanical gear.
- The first tested magnetic gear prototype was quieter when operating at rated speed and under sufficiently high partial load than a mechanical gear operating under the same conditions.
- The second tested magnetic gear prototype was louder when operating at rated speed and under partial load than the mechanical gear operating under the same conditions.
- This study is the first to demonstrate that a magnetic gear's radiated acoustic noise is load dependent. In particular, both magnetic gears became audibly quieter as their torque load increased; whereas the mechanical gear became audibly louder as its torque load increased.

ACKNOWLEDGMENT

Portions of this research were conducted with the advanced computing resources provided by Texas A&M High Performance Research Computing. The authors would like to thank ANSYS for their support of the EMPE lab through the provision of FEA software.

REFERENCES

[1] K. Kairouz and D. Price, "The differentiation of belt drive and direct drive fans for industrial processes", *Engineered Sys. Mag.*, Mar. 2019. [Online].

[2] T. Frandsen, N. Berg, R. Holm and P. O. Rasmussen, "Start-up problem with an induction machine and a permanent magnet gear," in *Proc. IEEE Energy Convers. Congr. Expo.*, 2014, pp. 1348-1355.

[3] A. Matthee, R. Wang, C. Agenbach, D. Els, M. Kamper, "Evaluation of a magnetic gear for air-cooled condenser applications," *IET Electr. Power. Appl.*, vol. 12, no. 5, pp. 677-683, Apr. 2018.

[4] J. J. Scheidler and V. M. Asnani, "A review of noise and vibration control technologies for rotorcraft transmissions," NASA Glenn Res. Center, Cleveland, OH, USA, Tech. Rep. GRC-E-DAA-TN32233, Aug. 2016

[5] B. Praslicka, M. C. Gardner, M. Johnson and H. A. Toliyat, "Review and analysis of coaxial magnetic gear pole pair count selection effects," *IEEE J. Emerg. Sel. Topics Power Electron*., vol. 10, no. 2, pp. 1813-1822, Apr. 2022.

[6] B. Praslicka, D. F. Knight, T. L. Stefanelli, N. Palmer, A. White, J. Jones, H. A. Toliyat, "Design and Analysis of an Axial Flux Coaxial Magnetic Gear with Balanced Axial Forces for Precision Aerospace Actuation Application," in *Proc. IEEE Energy Convers. Congr. Expo*., 2022, pp. 1-8.

[7] H. Y. Wong, H. Baninajar, B. W. Dechant, P. Southwick, and J. Z. Bird, "Experimentally Testing a Halbach Rotor Coaxial Magnetic Gear with 279Nm/L Torque Density," *IEEE Trans Energy Convers.*, early access.

[8] S. S. Nielsen, R. K. Holm, N. I. Berg, and P. O. Rasmussen. "Magnetically geared conveyor drive unit - an updated version," in *Proc. IEEE Energy Convers. Congr. and Expo*., 2020, pp. 285-292.

[9] C. J. Agenbach, D. N. J. Els, R.-J. Wang, and S. Gerber, “Force and vibration analysis of magnetic gears,” in *Proc. Int. Conf. Elec. Mach.*, 2018, pp. 752–758.
[10] S. S. Nielsen, H. Y. Wong, H. Baninajar, J. Z. Bird and P. O. Rasmussen, “Pole and segment combination in concentric magnetic gears: vibrations and acoustic signature,” *IEEE Trans. Energy Conv.*, vol. 37, no. 3, pp. 1644-1654, Sept. 2022.
[11] V. M. Asnani, J. J. Scheidler, and T. Tallerico, “Magnetic gearing research at NASA,” in *Proc. of AHS Intl. 74th Annual Forum*, 2018, pp. 1-14.
[12] K. K. Uppalapati and J. Z. Bird, “An iterative magnetomechanical deflection model for a magnetic gear,” *IEEE Trans. Magn.*, vol. 50, no. 2, pp. 245-248, Feb. 2014.
[13] S. Gerber and R. Wang, “Design and evaluation of a magnetically geared PM machine,” *IEEE Trans. Magn.*, vol. 51, no. 8, pp. 1-10, Aug. 2015.
[14] S. Korsgaard, A. Kjaer, S. Nielsen, L. Demsa and P. O. Rasmussen, “Acoustic noise analysis of a magnetically geared permanent magnet generator,” in *Proc. IEEE Energy Convers. Congr. Expo.*, 2019, pp. 717-723.
[15] J. Lee and J. Chang, “Analysis of the vibration characteristics of coaxial magnetic gear,” *IEEE Trans. Magn*., vol. 53, no. 6, pp. 1-4, June 2017.
[16] M. Kowol, J. Kołodziej, R. Gabor, M. Łukaniszyn, and M. Jagieła, “On-load characteristics of local and global forces in co-axial magnetic gear with reference to additively manufactured parts of modulator,” *Energies*, vol. 13, no. 12, pp. 1–18, Jun. 2020.
[17] S. Modaresahmadi, K. Li, W. B. Williams and J. Z. Bird, “Vibration analysis of the first stage of a multi-stage coaxial magnetic gearbox,” in *Proc. SoutheastCon*, 2018, pp. 1-8, doi: 10.1109/SECON.2018.8478981.
[18] J. Y. Lee and J. H. Chang, “Vibration and noise characteristics of coaxial magnetic gear according to low-speed rotor structure,” *Journal of Mechanical Science and Technology*, vol. 31, no. 6, pp. 1–4, 2017
[19] C. V. Pop, D. Fodorean, C. Husar, and C. Irimia, “Noise and vibration analysis of an in-wheel motor with integrated magnetic gear dedicated for light electric application,” in *Proc. Int. Conf. Mod. Power Sys.*, pp. 1–5, 2019.
[20] M. C. Gardner, B. Praslicka, M. Johnson and H. A. Toliyat, “Optimization of coaxial magnetic gear design and magnet material grade at different temperatures and gear ratios,” *IEEE Trans. Energy Conv.*, vol. 36, no. 3, pp. 2493-2501, Sept. 2021.
[21] S. Gerber and R. Wang, “Cogging torque definitions for magnetic gears and magnetically geared electrical machines,” *IEEE Trans. Magn.*, vol. 54, no. 4, pp. 1-9, Apr. 2018.
[22] M. C. Gardner and H. A. Toliyat, “Nonlinear analysis of magnetic gear dynamics using superposition and conservation of energy,” in *Proc. IEEE Int. Elec. Mach. and Drives Conf.*, 2019, pp. 210-217.
[23] M. Johnson, M. C. Gardner and H. A. Toliyat, “Design comparison of NdFeB and ferrite radial flux surface permanent magnet coaxial magnetic gears,” *IEEE Trans. Ind. Appl.*, vol. 54, no. 2, pp. 1254-1263, Mar.-Apr. 2018.
[24] M. C. Gardner, B. E. Jack, M. Johnson, and H. A. Toliyat, “Comparison of surface mounted permanent magnet coaxial radial flux magnetic gears independently optimized for volume, cost, and mass,” *IEEE Trans. Ind. Appl.*, vol. 54, no. 3, pp. 2237–2245, May/Jun. 2018.
[25] D. Z. Abdelhamid and A. M. Knight, “The effect of modulating ring design on induction machine with integrated magnetic gear torque,” in *Proc. IEEE Energy Convers. Congr. and Expo.*, 2017, pp. 1169-1174.
[26] M. Johnson, M. C. Gardner, H. A. Toliyat, S. Englebretson, W. Ouyang and C. Tschida, “Design, construction, and analysis of a large-scale inner stator radial flux magnetically geared generator for wave energy conversion,” *IEEE Trans. Ind. Appl.*, vol. 54, no. 4, pp. 3305-3314, July-Aug. 2018.
[27] S. Gerber and R. -J. Wang, “Analysis of the end-effects in magnetic gears and magnetically geared machines,” in *Proc. Int. Conf. Elec. Mach.*, 2014, pp. 396-402.
[28] D. Talebi *et al*., “Design of an Extremely Efficient, Rare-Earth Free, 5 kW Motor in a NEMA 210 Frame”, in *Proc. IEEE Energy Convers. Congr. Expo*, 2022, pp. 1-6.
[29] J. Zhou, S. Wenlei, and L. Cao, “Vibration and noise characteristics of a gear reducer under different operation conditions.” *J. Low Freq. Noise Vibr. Active Contr.*, vol. 38, no. 2, pp. 574-591, June 2019.
[30] Y. Chen, and A. Ishibashi, “Investigation of the noise and vibration of planetary gear drives,” in *Proc. ASME Int. Power Trans. and Gearing Conf.*, pp. 507-513, Sep., 2003.
[31] H. Baninajar, S. Modaresahmadi, H. Y. Wong, J. Z. Bird, W. Williams, and B. Dechant, "Experimental Evaluation of a 63.3:1 Dual-Stage Coaxial Magnetic Gear," *IEEE Trans.Energy Convers.*, early access.
[32] M. C. Gardner, M. Johnson, and H. A. Toliyat, “Performance Impacts of Practical Fabrication Tradeoffs for a Radial Flux Coaxial Magnetic Gear with Halbach Arrays and Air Cores,” in *Proc. IEEE Energy Convers. Congr. and Expo*, 2019, pp. 3129-3136.
[33] J. J. Schiedler, Z. A. Cameron, and T. F. Tallerico, “High Speed Testing of a High Efficiency Concentric Magnetic Gear”, in *Proc. Propulsion and Power Technical Meeting*, 2019, pp. 1-27.
[34] Neugart Complete Gearbox Catalog, Neugart GmbH, Kippenheim, Germany, 2022.
[35] D. K. Khare, *et al.*, “Experimental investigation on gear rattle noise reduction in passenger car,” in *Proc. SAE Noise and Vibration Conference and Exhibition*, Jun. 2019.